ACOUSTICS 2012

Displacement field of the membrane of condenser microphones at high frequencies: Improvement of analytical solution

T. Lavergne, S. Durand, M. Bruneau and N. Joly

Laboratoire d'acoustique de l'université du Maine, Bât. IAM - UFR Sciences Avenue Olivier Messiaen 72085 Le Mans Cedex 9
thomas.lavergne@univ-lemans.fr

Condenser microphones are reciprocal transducers whose properties (sensitivity, bandwidth and reliability) make them powerful measurement tools. For their common use under standard conditions they have been appropriately characterised for nearly thirty years. But nowadays, their miniaturisation (using MEMS processes) and their new uses for metrological purposes under non-standard conditions (i.e. in high frequency ranges, in gas mixtures, and at various static pressures and temperatures) require a much deeper characterisation with respect to these new uses. Though recent literature on this topic [J. Acoust. Soc. Am. 128(6), 3459-3477 (2010)] leads to satisfying results according to these new requirements, the analytical solution given is not always sufficiently precise to interpret phenomena and must be improved to characterise more accurately the displacement field of the membrane up to high frequencies (100 kHz). Thus, the aim of the work presented here is to propose an improved analytical solution (especially by taking into account more appropriately the finite surface corresponding to the holes in the backing electrode) and to deduce results of interest, in particular concerning metrology purposes.

1 Introduction

Condenser microphones have been appropriately characterised for decades for their common use under standard conditions. A much deeper characterisation as the one available previously is today required due to their the miniaturisation (using MEMS processes) and to their new uses for metrological purposes under non-standard conditions (i.e. in high frequency ranges, in gas mixtures, and at various static pressures and temperatures).

An analytical modeling, presented recently in a paper [1] starting up again with a previous one [2], which describes the behaviour of the diaphragm of electrostatic transducers, appears to be a convenient tool to analyse (more particularly) the effect of the holes in the backing electrode on the displacement field which can be highly non-uniform in the highest frequency range. Being concerned by the use of this analytical approach when low uncertainties on the behaviour of acoustic fields generated or measured by these transducers are required up to 100k Hz, accurate theoretical results could be obtained provided that the main geometrical parameters (namely here those characterising the air gap and the holes in the backing electrode) are accounted for in a realistic manner.

Thus, this paper aims at providing results from improvements in introducing in the calculation a more realistic shape to describe the geometry of each hole, even though this shape remains reduced to several punctual equivalent volume velocity "sources". Moreover, an extended shape which accounts for the flow through the holes and in the air gap is introduced, showing that accurate results can be obtained (here the displacement of the membrane and the sensitivity), which are more realistic than those presented in the paper mentioned above. Furthermore, numerical simulations are concerned with examining the behaviour of the acoustic velocity fields around the interface between the holes and the air gap in order to help interpreting the value of the parameters used in the analytic simulations, and experimental results, obtained using a laser scanning vibrometer, are presented and compared to the analytical results.

2 Basic formulation of the analytical modeling

The purpose of this section is to resume the basis of the modeling presented in the literature [1] in order to remind of how the presence of the holes and the peripheral slit are taken into account in the basic equations which govern the coupled fields which take place in each part of the microphone (membrane, air-gap, backchamber, holes, and peripheral slit).

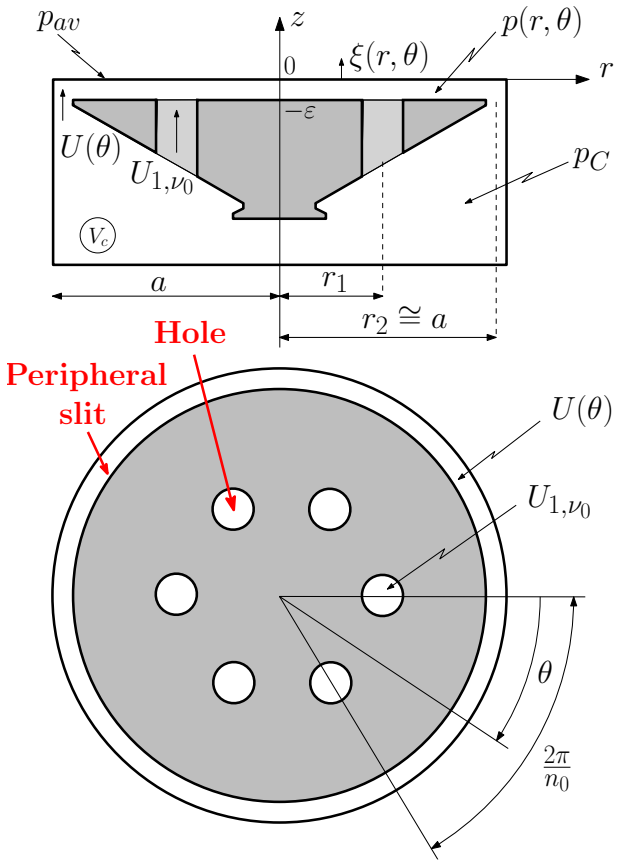

Figure 1: Diagram of a condenser microphone with 6 holes in the backing electrode.

The displacement field $\xi(r,\theta)$ of the membrane (see Figure 1), driven by a harmonic acoustic pressure p_{av} uniform over the surface (πa^2) and loaded by the pressure $p(r,\theta)$ in the air-gap, which is subjected to the Dirichlet boundary condition at its periphery ($r = a$), is governed by the following set of equations

$$T\left(\partial_{rr}^2 + \frac{1}{r}\partial_r + \frac{1}{r^2}\partial_{\theta\theta}^2 + K^2\right)\xi(r,\theta) = p_{av} - p(r,\theta), \quad \text{(1a)}$$

$$\xi(r=a,\theta) = 0, \quad \text{(1b)}$$

where $K = \omega\sqrt{M_s/T}$, and where ω, M_s and T are, respectively, the angular frequency, the mass per unit area, and the mechanical tension of the membrane.

In the air-gap between the membrane and the backing electrode, the pressure variation $p(r,\theta)$, which is assumed to be independent of the coordinate z (normal to the membrane), is governed by the following equation

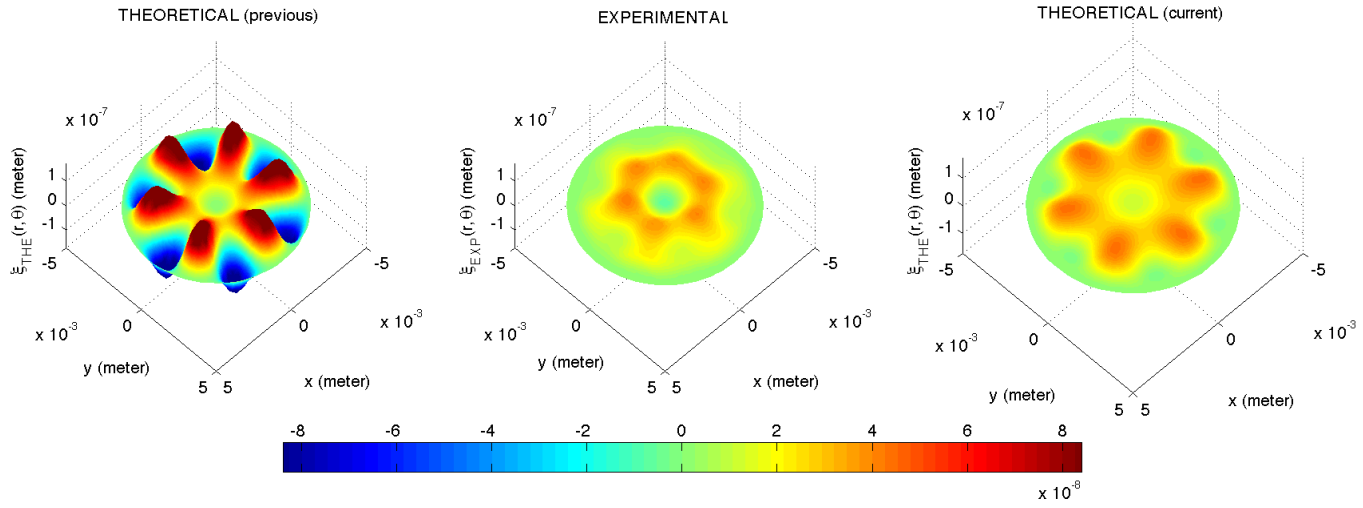

Figure 2: Displacement field of the membrane of a 1/2 in. B&K microphone type 4134 at 72 kHz.

$$\left(\partial_{rr}^2 + \frac{1}{r}\partial_r + \frac{1}{r^2}\partial_{\theta\theta}^2 + \chi^2\right) p(r,\theta) = -\frac{\rho_0\,\omega^2}{F_v}\,\frac{\xi(r,\theta)}{\varepsilon} - \frac{i\,\omega\,\rho_0}{F_v}\left[\sum_{\nu_0=1}^{n_0}\frac{U_{1,\nu_0}(r,\theta)}{\varepsilon}\,\frac{\delta(r-r_1)}{r}\,\delta(\theta-\theta_{\nu_0}) + \frac{U(\theta)}{\varepsilon}\,\frac{\delta(r-r_2)}{r}\right], \tag{2a}$$

with the Neumann boundary condition at the periphery (the radial component of the particle velocity vanishes $r \cong a$)

$$\partial_r p(r=a,\theta) = 0, \tag{2b}$$

where ε is the thickness of the air gap, ρ_0 the density of air, n_0 the number of holes in the backing electrode, δ is the Dirac function, r_1 and r_2 the distance between the centre of the membrane and, respectively, the centre of each hole and the centre of the peripheral slit, and where U_{1,ν_0} and $U(\theta)$ are the volume velocity of, respectively, the hole numbered μ_0 and the peripheral slit. The complex wavenumber χ and the function F_v account for the viscous and thermal boundary layers effects, assuming the no-slip condition and the isothermal boundary condition on the membrane and an approximate mixed boundary condition on the surface of the backing electrode involving its porosity (see details in [1, 3]). The first term in the right hand side of Eq. 2a represents the volume velocity of the diaphragm and shows the coupling between the displacement field $\xi(r,\theta)$ and the pressure field $p(r,\theta)$, and the second term represents the volume velocities (localized sinks) along the z-axis of each hole U_{1,ν_0} and of the peripheral slit $U(\theta)$. These volume velocities sources, which are assumed to be punctual (that is drastic an approximation), can be expressed as a function of the pressure variation in the air gap and the pressure variation in the backchamber as follows

$$U_{1,\nu_0} = y_{1,\nu_0}\,\left[\,p_C(r_1,\theta=0)) - p(r_1,\theta=0)\,\right], \tag{3a}$$

$$U(\theta) = y\,\left[\,p_C(r_2,\theta) - p(r_2,\theta)\right], \tag{3b}$$

where y_{1,ν_0} and y are the input admittance of each hole and of the peripheral slit respectively.

In the backchamber, the acoustic pressure field $p_C(r,\theta)$, which is subjected to Neumann boundary condition at the periphery ($r = a$), is governed by the following set of equations

$$\left(\partial_{rr}^2 + \frac{1}{r}\partial_r + \frac{1}{r^2}\partial_{\theta\theta}^2 + \chi_C^2\right) p_C(r,\theta) = \frac{i\,\omega\,\rho_0}{F_{vC}}\left[\sum_{\nu_0=1}^{n_0}\frac{U_{1,\nu_0}(r,\theta)}{\varepsilon_C}\,\frac{\delta(r-r_1)}{r}\,\delta(\theta-\theta_{\nu_0}) + \frac{U(\theta)}{\varepsilon_C}\,\frac{\delta(r-r_2)}{r}\right], \tag{4a}$$

$$\partial_r p_C(r=a,\theta) = 0, \tag{4b}$$

where ε_C is the average thickness of the backchamber, and where χ_C and F_{v_C} take into account the viscous and thermal boundary layers effects involving the porosity of the backing electrode.

This formulation leads to solutions, involving modal expansions on Dirichlet and Neumann eigenfunctions, which depend on the radial and the azimuthal coordinates, suitable to describe the intricate behaviour of the membrane in the highest frequency range.

3 Results and improvement of the analytical solution

The theoretical displacement field of the membrane shown in the left hand side of Figure 2 is obtained with the solution given in [1] and computed with the values of the geometrical, mechanical and electrical parameters given in [1, 2] for a 1/2 in. B&K microphone type 4134. The significant deviations appearing between this theoretical result and the experimental one (shown in the centre of Figure 2) may be due (at least partially) to the fact that the holes and the peripheral slit are modelled as Dirac "sources" localised at the centre of each hole and of the peripheral slit (punctual and linear sinks respectively). This approximation, although appropriate to describe the intricate behaviour of the membrane in the highest frequency range, is too drastic to characterize accurately the behaviour of the fluid in the air gap, and, consequently, the influence of the "sources" on the displacement field of the membrane. This is particularly true at certain frequencies (here 72 kHz) where the displacement field is highly non-uniform.

More accurate results can be obtained by accounting for more realistically the shape of the holes and the slit. Hence, each hole and the slit are described by, respectively, several punctual and several linear equivalent volume velocity "sources". The theoretical displacement field of the membrane shown in the right hand side of Figure 2 is obtained when the slit is described by two linear "sources" located at the coordinates $(r_2 - e/2)$ and (r_2) (e denoting the width of the slit), and when each hole is described by four punctual "sources" whose locations are on a radius of the microphone at the coordinates $(r_1 \pm R_1, \theta_{v_0})$ and between two holes at the coordinates $(r_1, \theta_{v_0} \pm d\theta)$ with $d\theta = atan(1.7R_1/r_1)$. It appears clearly that the theoretical displacement field of the membrane (calculated using this parameters) looks similar to the measured one, and to the one simulated in [4] (note that in this reference the displacement scale is not correct). Figure 3 shows the cross-sections of the three displacement fields represented on Figure 2 along a diameter passing through two holes. It is noteworthy that using the analytical solution presented here the amplitude of the displacement is quite well evaluated. However, the location of the maximum displacement does not correspond to the experimental one which is located (approximately) in front of the holes (i.e. for $r_1 \cong 2mm$) (actually this discrepancy depends on the approximated description of the extended "sources").

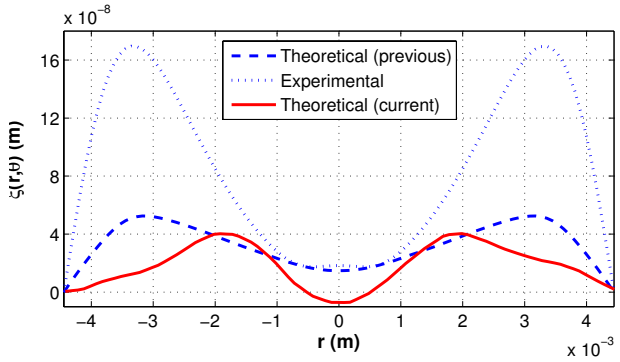

Figure 3: Cross-sections of the displacement fields shown on Figure 2.

The locations of the punctual and linear "sources" used here to describe the holes and the slit show that they behave as extended volume velocity "sources". To help us to understand the values of the parameters used (i.e. the locations of the "sources"), a numerical simulation accounting for the viscous and heat conduction effects in the boundary layers has been performed with an axisymetrical modelling using an anisotropic mesh [5] in order to examine the behaviour of the acoustic velocity fields around the interface between the holes and the air gap. In this axisymetrical simulation the holes in the backing electrode are replaced by an annular slit, whose surface corresponds to the total surface of the $n_0 = 6$ holes.

The result of the numerical simulation shown on Figure 4, obtained when considering an uniform velocity field of the membrane, represents the direction of the particle velocity (white arrows) and the amplitude of its axial component (color chart) at the mouth of the slit, on the side of the air gap.

It appears clearly that the amplitude of the axial velocity is maximum at the sharp edges of the slit. Thus, owing to this observation, it seems more appropriate to describe each holes by several punctual "sources" localised at the periphery of the holes instead of a single punctual "source" located at each of their centres. Note that the axial velocity is greater on the left side of Figure 4 (towards the centre of the membrane) than on the other side, so, in other words, the volume velocity "sources" do not have the same weight according to their locations (this should lead to theoretical results closer to the experimental one than that shown on Figures 2 and 3). Thus, to compensate the fact that the modelling [1] does not take this phenomenon into account the locations of the punctual "sources" would be rearranged according to their different weights.

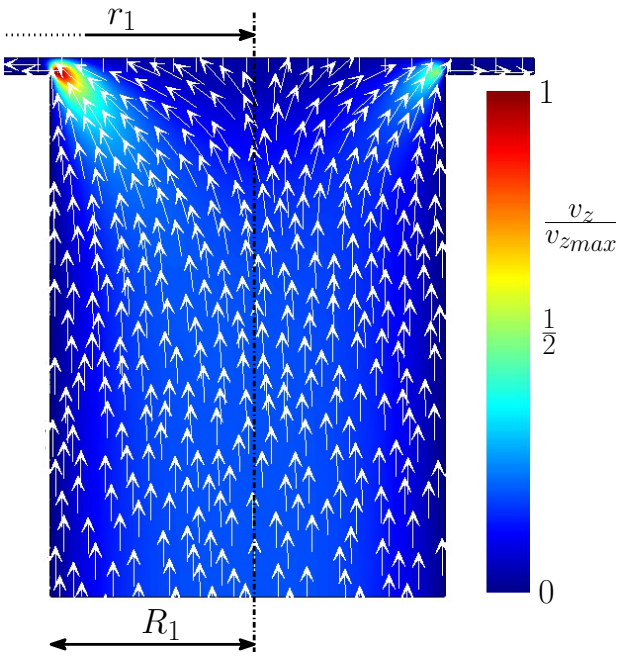

Figure 4: Axial component v_z of the particle velocity at 72 kHz (Arrows: Orientation of the particle velocity ; Colormap: Normalised magnitude of the axial component of the particle velocity).

4 Sensitivity of the microphone

The sensitivity as a function of the frequency (1/2 in. B&K microphone type 4134) obtained from the analytical procedure outlined in section 2, when modeling holes and peripheral slit as indicated in section 3, is shown in Figure 5 for the configuration outlined in table 1 and for the values of the parameters given in ref. [2], when considering one azimuthal mode ($m = 0$) and sixteen radial modes ($n = 0$ to 15) in the calculus: experimental result (upper curve, black solid line with dots), previous [1] theoretical result (lower curve red dotted line), current result (intermediate blue solid line).

As expected these results show clearly several features: first, the relatively good agreement between the current analytical result and the experimental one, especially concerning the very low frequency shift between the theoretical and experimental values of the resonance; second, the remaining discrepancies between the theoretical and experimental associated Q-factor which could be explained by the (unknown) uncertainties on the values of the geometrical, mechanical and electrical given in ref. [2]; third, the systematic lower theoretical level (−4 dB) which is currently non explained (it is the first time that such theoretical sensitivity curve is

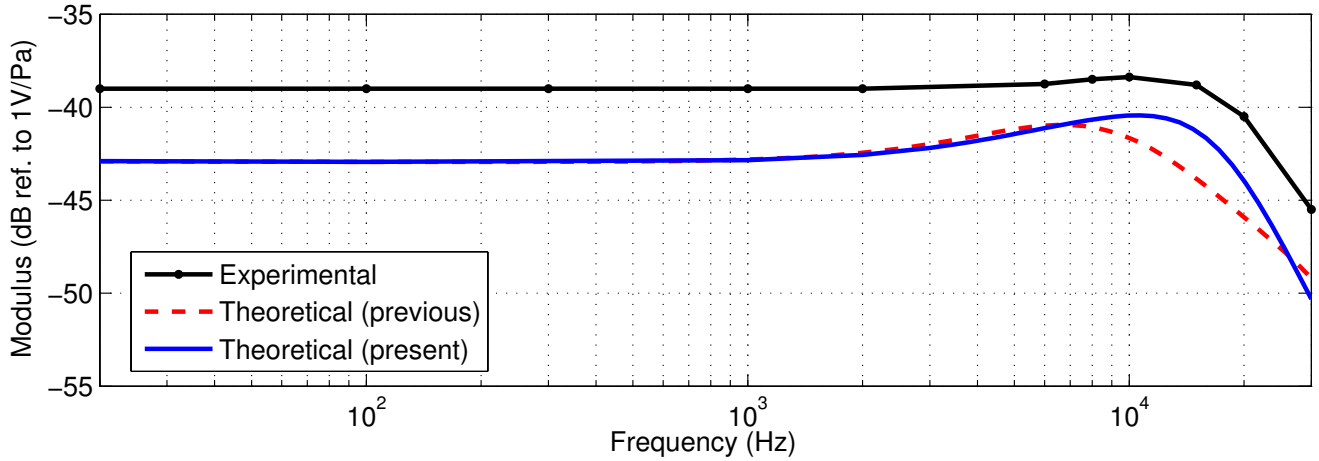

Figure 5: Sensitivity of the microphone vs frequency.

calculated from the geometrical, mechanical and electrical parameters).

Table 1: Values of the modified parameters used to compute the sensitivity shown on Figure 5 and of the parameters given in [2].

Parameter	Value from [2]	Value used here
Radius of a hole	$R_1 \cong 0.5$ mm	$R_1 \cong 0.5$ mm
Location of the punctual "sources"	$r_1 \cong 2$ mm	$r_1' = r_1 - R_1$ $r_1' \cong 1.5$ mm
Width of the peripheral slit	$a_2 \cong 0.84$ mm	$a_2 \cong 0.84$ mm
Location of the linear "source"	$r_2 \cong 4$ mm	$r_2' = r_2 - a_2/2$ $r_2' \cong 3.6$ mm

It is worth noting that non-linear effects which could appear around the sharp edges of the holes and the slit, namely separation of flow and even formation of vortices, could be non negligible for high incident pressure variation levels (they are not accounted for in the current modeling).

5 Conclusion

The aim of this study was to determine whether parameters adjusted to model the phenomena which occur around the holes in the air gap significantly improve results which can be obtained from an analytic approach recently published. The results gathered are consistent with this hypothesis, the conclusive numerical and experimental results (including those available recently in the literature [3]) confirming that. Further researches will consider other geometrical, mechanical, and electrical parameters and the use of the model in real situations concerning miniaturization and/or metrological applications. It is noteworthy that the theoretical results convey an interpretation of the physical phenomena, and that, while the analytical modelling presented here could appear somewhat cumbersome, the numerical calculations are in fact very simple and rapid to handle.

References

[1] T. Lavergne, S. Durand, M. Bruneau, D. Rodrigues and N. Joly, "Dynamic behavior of the circular membrane of an electrostatic microphone: Effect of holes in the backing electrode", *J. Acoust. Soc. Am.* **128**(6), 3459-3477 (2010)

[2] A.J. Zuckerwar, "Theoretical response of condenser microphones", *J. Acoust. Soc. Am.* **64**(5), 1278-1285 (1978)

[3] R.S. Grinnip, "Advanced Simulation of a Condenser Microphone Capsule", *J. Aud. Eng. Soc.* **54**(3), 157 166 (2006)

[4] D. Homentcovschi, R.N. Miles , "An analytical-numerical method for determining the mechanical response of a condenser microphone", *J. Acoust. Soc. Am.* **130**(6), 3698-3705 (2011)

[5] N. Joly, "Finite Element Modeling of Thermoviscous Acoustics on Adapted Anisotropic Meshes: Implementation of the Particle Velocity and Temperature Variation Formulation", *Acta Acustica united with Acustica* **96**, 102-114 (2010)